

LETTER TO THE EDITOR

# *Herschel* measurements of the D/H and $^{16}\text{O}/^{18}\text{O}$ ratios in water in the Oort-cloud comet C/2009 P1 (Garradd)<sup>★</sup>

D. Bockelée-Morvan<sup>1</sup>, N. Biver<sup>1</sup>, B. Swinyard<sup>2,3</sup>, M. de Val-Borro<sup>4</sup>, J. Crovisier<sup>1</sup>, P. Hartogh<sup>4</sup>, D.C. Lis<sup>5</sup>, R. Moreno<sup>1</sup>, S. Szutowicz<sup>6</sup>, E. Lellouch<sup>1</sup>, M. Emprechtinger<sup>5</sup>, G.A. Blake<sup>5</sup>, R. Courtin<sup>1</sup>, C. Jarchow<sup>4</sup>, M. Kiderger<sup>7</sup>, M. Küppers<sup>7</sup>, M. Rengel<sup>4</sup>, G.R. Davis<sup>8</sup>, T. Fulton<sup>9</sup>, D. Naylor<sup>9</sup>, S. Sidher<sup>3</sup>, and H. Walker<sup>3</sup>

(Affiliations can be found after the references)

Received

## ABSTRACT

The D/H ratio in cometary water is believed to be an important indicator of the conditions under which icy planetesimals formed and can provide clues to the contribution of comets to the delivery of water and other volatiles to Earth. Available measurements suggest that there is isotopic diversity in the comet population. The *Herschel* Space Observatory revealed an ocean-like ratio in the Jupiter-family comet 103P/Hartley 2, whereas most values measured in Oort-cloud comets are twice as high as the ocean D/H ratio. We present here a new measurement of the D/H ratio in the water of an Oort-cloud comet. HDO, H<sub>2</sub>O, and H<sub>2</sub><sup>18</sup>O lines were observed with high signal-to-noise ratio in comet C/2009 P1 (Garradd) using the *Herschel* HIFI instrument. Spectral maps of two water lines were obtained to constrain the water excitation. The D/H ratio derived from the measured H<sub>2</sub><sup>16</sup>O and HDO production rates is  $(2.06 \pm 0.22) \times 10^{-4}$ . This result shows that the D/H in the water of Oort-cloud comets is not as high as previously thought, at least for a fraction of the population, hence the paradigm of a single, archetypal D/H ratio for all Oort-cloud comets is no longer tenable. Nevertheless, the value measured in C/2009 P1 (Garradd) is significantly higher than the Earth's ocean value of  $1.558 \times 10^{-4}$ . The measured  $^{16}\text{O}/^{18}\text{O}$  ratio of  $523 \pm 32$  is, however, consistent with the terrestrial value.

**Key words.** Comets: general; Comets: individual: C/2009P1 (Garradd); Submillimeter: planetary systems; Oort cloud; Astrochemistry

## 1. Introduction

Having retained and preserved pristine material from the solar nebula, comets contain unique clues to the history and evolution of the solar system (Irvine et al., 2000). Isotopic ratios are important indicators of the conditions under which cometary materials formed, since isotopic fractionation is very sensitive to physical conditions. In addition, the characterization of the isotopic composition of long-period comets from the Oort cloud and of short-period comets from the Jupiter family can provide clues to their formation regions in the early solar system.

The D/H ratio in water has been determined in several Oort-cloud comets (OCC) using different techniques, with most measurements agreeing with a value of  $\sim 3 \times 10^{-4}$  (Jehin et al., 2009, and references therein). In addition, the ratio was measured using the ESA *Herschel* Space Observatory (Pilbratt et al., 2010) in the Jupiter-family comet (JFC) 103P/Hartley 2 (Hartogh et al., 2011), where it was found to be  $(1.61 \pm 0.24) \times 10^{-4}$ , i.e., consistent with the Vienna standard mean ocean water (VSMOW) value equal to  $1.558 \times 10^{-4}$ . This result was unexpected. Models quantifying the deuterium enrichment factor in the solar nebula with respect to the protosolar value predicted an increase in the D/H ratio with increasing heliocentric distance (e.g., Hersant et al., 2001; Kavelaars et al., 2011). According to the most accepted theory, OCCs and JFCs originate from the same population of objects formed in the Uranus-Neptune zone (Dones et al., 2004), though part of the Oort cloud was possibly formed by planetesimals scattered from the Jupiter-Saturn region

(Brasser, 2008). Therefore, JFCs were expected to exhibit a D/H ratio similar to or higher than that in OCCs (Kavelaars et al., 2011).

We present in this paper a new measurement of the D/H ratio in the water of an Oort-cloud comet, obtained with the same instrumentation and methodology as those used for comet 103P/Hartley 2. Comet C/2009 P1 (Garradd) was observed with the Heterodyne Instrument for the Far-Infrared (HIFI, de Graauw et al., 2010) in the framework of the *Herschel* guaranteed time key programme “Water and related chemistry in the solar system” (Hartogh et al., 2009).

## 2. Observations

Comet C/2009 P1 (Garradd) is a long-period comet originating from the Oort cloud ( $P = 127\,000$  yr, orbit inclination of  $106^\circ$  with respect to the ecliptic; Nakano, 2012). Discovered on 13 August 2009 at a heliocentric distance  $r_h = 8.7$  AU (McNaught & Garradd, 2009), it passed perihelion on 23 December 2011 at  $r_h = 1.55$  AU. The HDO observations with the HIFI instrument were performed on 6 October 2011, when the comet was at  $r_h = 1.88$  AU, and a distance from *Herschel* of 1.76 AU. The H<sub>2</sub><sup>18</sup>O and H<sub>2</sub>O lines were observed simultaneously. Since the H<sub>2</sub>O ground state rotational lines in comets are optically thick (Bensch & Bergin, 2004; Zakharov et al., 2007), lines of the rare oxygen isotopic counterpart H<sub>2</sub><sup>18</sup>O should, in principle, provide a more reliable reference for the D/H determination.

The observing sequence followed the same scheme as that used for comet 103P/Hartley 2 (Hartogh et al., 2011). It consisted of ten 30-min long observations of the HDO 1<sub>10</sub>-1<sub>01</sub> rotational line at 509.292 GHz, interleaved with 6-min simulta-

<sup>★</sup> *Herschel* is an ESA space observatory with science instruments provided by European-led principal investigator consortia and with important contribution from NASA.

**Table 1.** HIFI observations of C/2009 P1 (Garrad) on 6 October 2011. Spectra characteristics and production rates.

Line	$\nu$ (GHz)	Mode	Date <sup>a</sup> (Oct. UT)	Line area <sup>b</sup> (mK km s <sup>-1</sup> )	$\Delta\nu$ (m s <sup>-1</sup> )	Production rate <sup>i</sup>			
						$T_{\text{law}}$	$T_{\text{kin}} = 25 \text{ K}$ (s <sup>-1</sup> )	$T_{\text{kin}} = 47 \text{ K}$	
HDO	1 <sub>10</sub> -1 <sub>01</sub>	509.29242	Single-point	6.428 <sup>c</sup>	22.5 ± 2.0	-59 ± 33	9.8(±0.9)	9.2(±0.9)	7.7(±0.6) × 10 <sup>25</sup>
H <sub>2</sub> <sup>18</sup> O	1 <sub>10</sub> -1 <sub>01</sub>	547.67644	Single-point	6.415 <sup>d</sup>	179 ± 5	-21 ± 13	4.55(±0.12)	4.97(±0.12)	3.94(±0.11) × 10 <sup>26</sup>
H <sub>2</sub> O	1 <sub>10</sub> -1 <sub>01</sub>	556.93600	Single-point	6.415 <sup>d</sup>	9318 ± 12	320 ± 2	23.8(±0.6)	23.4(±0.6)	16.5(±0.4) × 10 <sup>28</sup>
H <sub>2</sub> O	1 <sub>10</sub> -1 <sub>01</sub>	556.93600	Mapping	6.291 <sup>e</sup>	8897 ± 98 <sup>h</sup>	331 ± 20 <sup>h</sup>	23.2(±1.6)	26.2(±4.0)	20.8(±5.5) × 10 <sup>28</sup>
H <sub>2</sub> O	1 <sub>10</sub> -1 <sub>01</sub>	556.93600	Mapping	6.559 <sup>f</sup>	8109 ± 82 <sup>h</sup>	293 ± 16 <sup>h</sup>	21.4(±1.8)	24.1(±3.7)	19.2(±5.0) × 10 <sup>28</sup>
H <sub>2</sub> O	2 <sub>02</sub> -1 <sub>11</sub>	987.92676	Mapping	6.597 <sup>g</sup>	7140 ± 198 <sup>h</sup>	21 ± 19 <sup>h</sup>	18.2(±1.0)	20.6(±2.1)	15.5(±2.8) × 10 <sup>28</sup>

**Notes.** (a) Mean date. (b) Average of HRS and WBS line area retrievals in main-beam brightness-temperature scale  $T_{\text{mb}}$ . The error bar corresponds to statistical noise, which is multiplied by 1.5 for single-point observations observed in FSW mode to account for uncertainties in the baseline removal. (c) Herschel observation identification number (Obsid) 1342230#, with # = 187, 189, 191, 193, 195, 197, 199, 201, 203, and 205. (d) Obsid: # = 186, 188, 190, 192, 194, 196, 198, 200, 202, and 204. (e) Obsid: #185. (f) Obsid: #206. (g) Obsid: #209. (h) From the average of spectra within 10'' of the peak brightness. (i) For single-point data, a 4'' beam offset is considered (Appendix A). For mapping data, the production rate corresponds to the weighted mean of apparent production rates measured over the whole map, and the error bar is the dispersion around the mean.

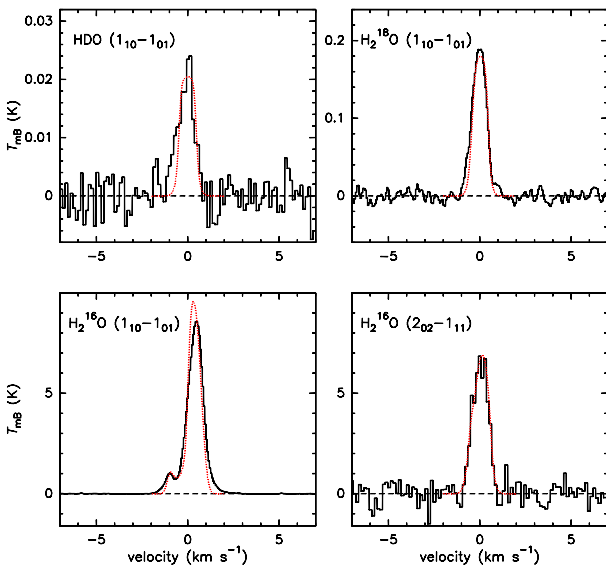


**Fig. 1.** HIFI spectra of comet C/2009 P1 (Garrad) observed on 6 October 2011 with the HRS. HDO (509 GHz), H<sub>2</sub>O (557 GHz), and H<sub>2</sub><sup>18</sup>O (548 GHz) 1<sub>10</sub>-1<sub>01</sub> spectra are the average of single-point measurements. The spectrum of the H<sub>2</sub>O 2<sub>02</sub>-1<sub>11</sub> line at 988 GHz is extracted from the map, by averaging data at offsets < 10'' from the peak. The velocity scale is given with respect to the comet rest frame. Synthetic line profiles obtained with 30% extended production (see text) are shown by red dotted lines. Gas acceleration (velocity increasing from 0.48 km s<sup>-1</sup> to 0.58 km s<sup>-1</sup> from  $r = 10^4$  km to  $10^5$  km) is considered to fit more closely the wings of the profiles (Combi et al., 2004).

neous measurements of the H<sub>2</sub>O and H<sub>2</sub><sup>18</sup>O 1<sub>10</sub>-1<sub>01</sub> ortho lines at 556.936 GHz and 547.676 GHz, respectively. In addition to these single-point measurements, two on-the-fly maps of the H<sub>2</sub>O 1<sub>10</sub>-1<sub>01</sub> transition (of 16-min duration) were acquired at the beginning and end of the sequence. Finally, a map of the H<sub>2</sub>O 2<sub>02</sub>-1<sub>11</sub> para transition at 987.926 GHz was performed with an integration time of 25 min. The full sequence spanned 6.85–14.71 UT on 6 October, with the maps serving to constrain the H<sub>2</sub>O excitation (Hartogh et al., 2010; de Val-Borro et al., 2010).

The H<sub>2</sub>O and H<sub>2</sub><sup>18</sup>O 1<sub>10</sub>-1<sub>01</sub> lines were observed in the upper and lower sidebands of the HIFI band 1a mixer, respectively. The

HDO line was also observed with the band 1a mixer, whereas data on the H<sub>2</sub>O 2<sub>02</sub>-1<sub>11</sub> line at 988 GHz were acquired using the band 4a mixer. The single-point observations were carried out in the frequency-switching mode (FSW) with a frequency throw of 94.5 MHz. On-the-fly 557 GHz and 988 GHz maps were acquired using Nyquist sampling, and spatial coverages of 4'×4' and 2'×2', respectively. The observing mode for the maps used a reference position at 10' from the comet in RA. Spectra were acquired with both the Wideband Spectrometer (WBS) and High Resolution Spectrometer (HRS). The spectral resolution of the WBS is 1.1 MHz. The HRS was used either in high-resolution (125 kHz) or nominal-resolution mode (250 kHz), enabling us to sample the line shapes at a spectral resolution of 70–150 m s<sup>-1</sup>. The telescope beam sizes at the frequencies of the three lines observed in band 1a are similar (half-power beam widths of 38''1, 38''7, and 41''6 for the H<sub>2</sub>O, H<sub>2</sub><sup>18</sup>O, and HDO lines, respectively), so that the three molecules were observed over the same (~ 55 000 km diameter) region of the coma.

Figure 1 shows the HRS spectra of the single pointing measurements (HDO, H<sub>2</sub>O, and H<sub>2</sub><sup>18</sup>O 1<sub>10</sub>-1<sub>01</sub> lines), as well as the H<sub>2</sub>O 2<sub>02</sub>-1<sub>11</sub> spectrum extracted from the central part of the map. Data reduction and calibration uncertainties are discussed in Appendix A. The HDO line is detected with a line-integrated signal-to-noise ratio of 17. Maps are shown in Fig 2. Line intensities and velocity offsets ( $\Delta\nu$ ) in the comet rest-frame are given in Table 1. The H<sub>2</sub>O 1<sub>10</sub>-1<sub>01</sub> line at 557 GHz is optically thick and has an asymmetric profile owing to self-absorption in the foreground coma. Intensity variations with time of up to 7% are observed for this line, which is related to intrinsic comet variability or instrumental effects. Optically thin HDO and H<sub>2</sub><sup>18</sup>O lines have approximately symmetric profiles. As the phase angle was 32°, the small negative-velocity offset observed for these lines suggests a modest excess of outgassing toward the Sun.

### 3. Analysis

The analysis was carried out using one-dimensional excitation models of HDO, H<sub>2</sub>O, and H<sub>2</sub><sup>18</sup>O (Biver et al., 2007). Models include collisions with H<sub>2</sub>O and electrons, which dominate the excitation in the inner coma, and solar infrared pumping of vibrational bands followed by spontaneous decay, which establishes fluorescence equilibrium in the outer coma. Radiation trapping strongly affects H<sub>2</sub>O excitation and is considered using the escape probability formalism. Consistent results were obtained using state-of-the-art radiation transfer methods (Hartogh et al.,

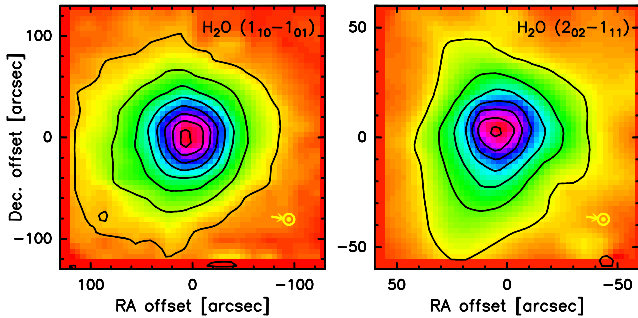


**Fig. 2.** On-the-fly maps of  $\text{H}_2\text{O}$  in C/2009 P1 (Garrad) obtained with the WBS. Left: the  $1_{10}-1_{01}$  557 GHz line observed on 6.291 October 2011 UT. Right: the  $2_{02}-1_{11}$  line at 988 GHz observed on 6.597 October 2011 UT. The contour spacing is  $1 \text{ K s}^{-1}$  in brightness temperature, corresponding to  $\sim 6\sigma$ . The Sun direction is indicated at lower right. The beam sizes are  $38''.1$  and  $21''.5$  at 557 GHz and 988 GHz, respectively.

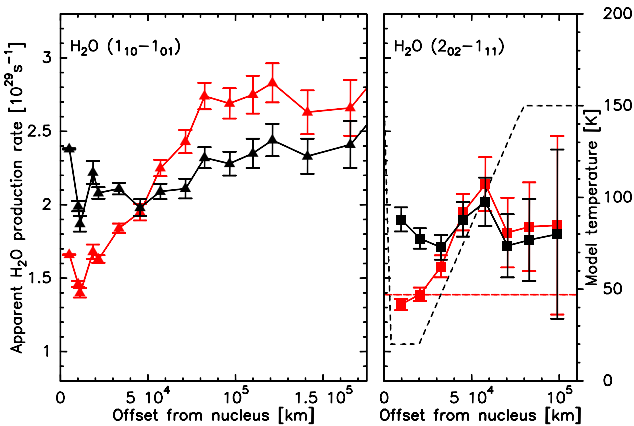


**Fig. 3.** Apparent  $\text{H}_2\text{O}$  production rates as a function of beam offset deduced from the 557 GHz (left) and 988 GHz (right)  $\text{H}_2\text{O}$  maps observed on 6.56 and 6.60 October UT, respectively. Calculations with a 47 K and variable  $T_{\text{kin}}$  are shown with red and black symbols, respectively. The temperature profiles are plotted in the right panel with dashed lines.

2010; Bensch & Bergin, 2004; Zakharov et al., 2007). Synthetic spectra are then computed using radiative transfer modelling. We assumed isotropic outgassing at a constant velocity. The model input parameters are: i) the gas expansion velocity, assumed to be  $0.6 \text{ km s}^{-1}$ , corresponding to the half widths of optically thin HDO,  $\text{H}_2\text{O}$  (988 GHz), and  $\text{H}_2^{18}\text{O}$  lines; ii) the gas temperature profile; iii) the  $x_{\text{ne}}$  scaling factor of the electron density profile, taken to be equal to 0.2 (Biver et al., 2007; Hartogh et al., 2010; de Val-Borro et al., 2010). The  $\text{H}_2\text{O}$  ortho-to-para ratio is assumed to be 3.

Line intensities for spectra probing the inner coma are sensitive to the gas temperature profile, which controls both the population of the rotational levels and the optical depth of the lines. Hence, the evolution of the intensity of the  $\text{H}_2\text{O}$   $1_{10}-1_{01}$  and  $2_{02}-1_{11}$  lines with beam offset,  $\rho$  (km), carries information about the temperature profile. Figure 3 presents the apparent  $\text{H}_2\text{O}$  production rate  $Q_{\text{app}}(\text{H}_2\text{O})$  as a function of  $\rho$  deduced from the maps. With appropriate modelling, the  $Q_{\text{app}}$  curve should be flat, if the nucleus is the dominant source of water vapour with a constant outgassing rate. Figure 3 presents the results for  $T_{\text{kin}} = 47 \text{ K}$ , a value consistent with multi-line observations of methanol undertaken with the IRAM 30-m telescope

in September and October 2011 with a  $17''$  beam comparable to the HIFI beam (Biver et al., 2012). For both lines,  $Q_{\text{app}}(\text{H}_2\text{O})$  increases with increasing  $\rho$  for a constant temperature profile. Deviations from constant  $Q_{\text{app}}(\text{H}_2\text{O})$  are enhanced when using  $x_{\text{ne}} > 0.2$  (Hartogh et al., 2010). The temperature law  $T_{\text{law}}$  that minimizes the deviations of  $Q_{\text{app}}(\text{H}_2\text{O})$  from a constant value, and provides consistent (within 15%) water production retrievals from the two lines, has a minimum of 20 K at a distance  $r = 4-20 \times 10^3 \text{ km}$  from the nucleus (thereby increasing the self-absorption and  $Q_{\text{app}}$  values) and then increases up to 150 K at  $r = 8 \times 10^4 \text{ km}$  (Fig. 3). This temperature increase may be related to the increased efficiency of photolytic heating (Combi et al., 2004). We note that the line intensities are weakly sensitive to the temperature at  $r < 1000 \text{ km}$  and  $r > \text{a few } 10^4 \text{ km}$ . The velocity offsets  $\Delta v$  of the on-nucleus synthetic 557(988) GHz line profiles are  $+292 (+50)$  and  $+259 (+39) \text{ m s}^{-1}$ , for  $T_{\text{law}}$  and  $T_{\text{kin}} = 47 \text{ K}$ , respectively. Hence, the model with a variable temperature also fits more closely the large positive  $\Delta v$  of the central 557 GHz spectra ( $+320 \text{ m s}^{-1}$ , Table 1), as it enhances the optical thickness of the line.

We examined whether the increase in  $Q_{\text{app}}(\text{H}_2\text{O})$  with  $\rho$  obtained with constant  $T_{\text{kin}}$  could instead be attributed to water production from icy grains in the outer coma. For  $T_{\text{kin}} = 47 \text{ K}$ , we are able to obtain a flat  $Q_{\text{app}}(\text{H}_2\text{O})$  profile for the 557 GHz line when assuming that 90% of water production is extended with a characteristic Haser scale-length of  $L_{\text{ext}} = 30000 \text{ km}$ . However this model is unsatisfactory since: i) the apparent production rate given by the 988 GHz line now decreases with increasing  $\rho$ ; 2) the predicted  $\Delta v$  of the 557 GHz line is 30% lower than observed; 3) the inferred  $^{16}\text{O}/^{18}\text{O}$  ratio in water is then three times lower than the Earth value. On the other hand, subliming icy grains were possibly present in C/2009 P1 (Garrad)'s coma (Paganini et al., 2012). We therefore considered an alternative model with moderate (30%) water production from long-lived icy grains (model outputs are insensitive to an unresolved source of water). This model explains the water 557 and 987 GHz maps for  $L_{\text{ext}} = 50000 \text{ km}$  and a temperature law similar to  $T_{\text{law}}$  (minimum of 20 K at  $r = 4-16 \times 10^3 \text{ km}$ ). The retrieved production rates and production rate ratios are identical (within 3%) to those found for nuclear production with  $T_{\text{law}}$ . This model accounts satisfactorily for the observed line profiles (Fig. 1).

Table 1 presents the production rates calculated with  $T_{\text{law}}$ , along with those for constant  $T_{\text{kin}} = 25 \text{ K}$  and  $47 \text{ K}$ . To compute the error bars in the production rate and isotopic ratios (derived from the simultaneous single-point data), we take into account a 5% relative calibration uncertainty (Appendix A). Using  $T_{\text{law}}$ , the  $\text{HDO}/\text{H}_2^{18}\text{O}$  production rate ratio is  $0.215 \pm 0.023$ . This is significantly larger than the value  $0.161 \pm 0.017$  measured for 103P/Hartley 2 (Hartogh et al., 2011). For  $T_{\text{kin}} = 25 \text{ K}$  and  $47 \text{ K}$ , one finds  $\text{HDO}/\text{H}_2^{18}\text{O} = 0.185$  and  $0.195 (\pm 0.020)$ , respectively, hence the retrievals are only slightly temperature-dependent.

The  $\text{H}_2^{16}\text{O}/\text{H}_2^{18}\text{O}$  production rate ratios derived from the band 1a observations using  $T_{\text{kin}} = 47 \text{ K}$  is  $419 \pm 26$ , while for  $T_{\text{law}}$  and  $T_{\text{kin}} = 25 \text{ K}$  one finds  $523 \pm 32$  and  $470 \pm 29$ , respectively. These latter values are in good agreement with previous measurements in comets (Jehin et al., 2009, and references therein), as well as with the  $^{16}\text{O}/^{18}\text{O} = 498.7 \text{ VSMOW}$  value, giving further confidence that our radiation-transfer model properly accounts for the opacity of the  $\text{H}_2^{16}\text{O}$  lines, provided a low gas temperature is adopted.

We adopt the model with  $T_{\text{law}}$  for the determination of the D/H ratio, as it best explains the  $\text{H}_2\text{O}$  maps and line profiles. The D/H measurement for 103P/Hartley 2 was based on the  $\text{HDO}/\text{H}_2^{18}\text{O}$  ratio (Hartogh et al., 2011), assuming  $^{16}\text{O}/^{18}\text{O} =$

$500 \pm 50$ . Using the same method, we derive  $\text{D}/\text{H} = (2.15 \pm 0.32) \times 10^{-4}$  for C/2009 P1 (Garrad). Using instead directly the  $\text{HDO}/\text{H}_2^{16}\text{O}$  production-rate ratio results in  $\text{D}/\text{H} = (2.06 \pm 0.22) \times 10^{-4}$ . This value will be adopted for the discussion. We note that consistent results are derived using constant (25–47 K) gas temperatures and 30% extended production (central values ranging from  $1.96$  to  $2.33 \times 10^{-4}$ ).

The water production rate derived using  $T_{\text{law}}$  is in the high range of values measured by other techniques in October 2011 (see discussion in Appendix B). Using a lower value would imply that the water of C/2009 P1 (Garrad) is highly enriched in  $^{18}\text{O}$  relative to both the Sun and all rocky bodies of the inner solar system (McKeegan et al., 2011). On the other hand, only an extreme  $^{18}\text{O}$  enrichment ( $^{16}\text{O}/^{18}\text{O}$  ratio of  $\sim 330$ , i.e.,  $\delta^{18}\text{O} = +500$  ‰ in geochemical notation) would reconcile the D/H ratio in comet C/2009 P1 (Garrad) with the canonical Oort-cloud value of  $3 \times 10^{-4}$ . Such high  $^{18}\text{O}$  enrichments have not been found so far in any solar system body (McKeegan et al., 2011), except for CO in the Titan’s atmosphere (Courtin et al., 2011). Our preferred interpretation is thus that the  $^{16}\text{O}/^{18}\text{O}$  ratio in comet Garrad is consistent with the VSMOW value.

#### 4. Discussion

The discovery of a D/H value equal to that of the Earth’s oceans in the Jupiter-family comet 103P/Hartley 2 showed that the reservoir of Earth-like water in the solar system is substantially larger than previously thought, including now both carbonaceous meteorites and comets (Hartogh et al., 2011). It also revealed that isotopic diversity is present in the comet population, with members of the Oort cloud having a deuterium enrichment of up to a factor of two with respect to VSMOW (Fig. 4). As discussed by Hartogh et al. (2011), the suggested dichotomy between Oort-cloud and Jupiter-family comets is difficult to explain in the context of current models predicting deuterium enrichments in cometary ices, and, if real, would imply to revisit the source regions of OCCs and JFCs. Actually, the only dynamical theory that could explain in principle an isotopic dichotomy in D/H is the one arguing that a substantial fraction of Oort-cloud comets were captured from other stars when the Sun was in its birth cluster (Levison et al., 2010).

The paradigm for a single, archetypal D/H ratio for all Oort-cloud comets is no longer tenable. The value of  $(2.06 \pm 0.22) \times 10^{-4}$  measured in comet C/2009 P1 (Garrad) is smaller than the mean of previous determinations in Oort-cloud comets ( $(2.96 \pm 0.25) \times 10^{-4}$ , Hartogh et al., 2011), and is consistent with the upper limit of  $2.5 \times 10^{-4}$  measured in comet 153P/Ikeya-Zhang (Fig. 4, Biver et al., 2006). We note that Brown et al. (2012) reexamined mass-spectrometer measurements for 1P/Halley (Eberhardt et al., 1995), reevaluating this value to be  $2.1 \times 10^{-4}$ . Altogether, the available data suggest that the deuterium enrichment in the water of Oort-cloud comets is not as high as previously thought, at least for a fraction of the population. Nevertheless, the D/H ratio measured in comet C/2009 P1 (Garrad) is significantly higher (by  $2.3 \sigma$ ) than the VSMOW value measured in 103P/Hartley 2. Interestingly, the range of D/H ratios measured in Stardust samples from comet 81P/Wild 2 (McKeegan et al., 2006) is the same as measured in the bulk water of various comets.

Dynamical modelling suggests that the distribution of planetesimals underwent large-scale mixing during the stages of planetary migration (Walsh et al., 2011). Therefore, variations in the cometary D/H may be expected within each population, if ancestor reservoirs were isotopically different. Isotopic diversity may be linked to the large compositional diversity observed

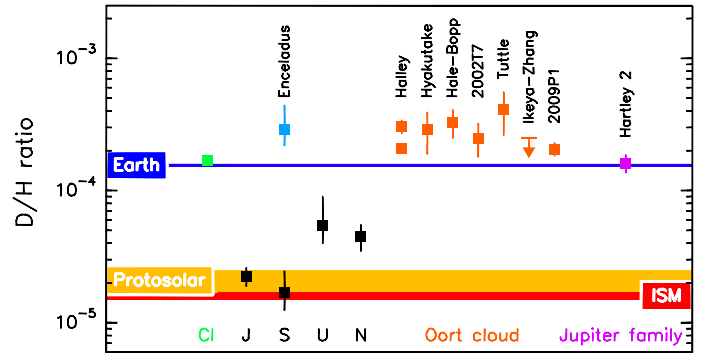


**Fig. 4.** D/H ratio in the water of comets (including the revised value for Halley from Brown et al. (2012)) compared to values in carbonaceous meteorites (CI), the Earth’s oceans, and Enceladus. Displayed data for planets, interstellar medium (ISM), and the protosolar nebula refer to the value in  $\text{H}_2$ . Adapted from Hartogh et al. (2011).

within both OCC and JFC populations (Bockelée-Morvan, 2011). Finally, experimental studies of ice sublimation suggest that the D/H measured in the evaporated vapour might be enhanced or depleted with respect to the bulk D/H in the cometary nucleus (Brown et al., 2012). This demonstrates the need to increase the sample of comets with accurate measurements of the D/H ratio, as well as perform further modelling.

*Acknowledgements.* HIFI has been designed and built by a consortium of institutes and university departments from across Europe, Canada and the United States (NASA) under the leadership of SRON, Netherlands Institute for Space Research, Groningen, The Netherlands, and with major contributions from Germany, France and the US. Support for this work was provided by NASA through an award issued by JPL/Caltech. SS was supported by polish MNiSW funds (181/N-HSO/2008/0).

#### References

- Bensch, F., & Bergin, E. A. 2004, *ApJ*, 615, 531  
 Biver, N., Bockelée-Morvan, D., Crovisier, J., et al. 2006, *A&A*, 449, 1255  
 Biver, N., Bockelée-Morvan, D., Crovisier, J., et al. 2007, *Planet. Space Sci.*, 55, 1058  
 Biver, N., Bockelée-Morvan, D., Lis, D.C., et al. 2012, *Asteroids, Comets, Meteors 2012*, 16–20 May 2012, Niigata, Japan  
 Bockelée-Morvan, D. 2011, *IAU Symposium*, 280, 261  
 Brasser, R. 2008, *A&A*, 492, 251  
 Brown, R. H., Lauretta, D. S., Schmidt, B., & Moores, J. 2012, *Planet. Space Sci.*, 60, 166  
 Colom, P., Crovisier, J., Biver, N., & Bockelée-Morvan, D. 2011, *EPSC-DPS Joint Meeting 2011*, 837  
 Combi, M. R., Harris, W. M., & Smyth, W. H. 2004, *Comets II*, 523  
 Courtin, R., Swinyard, B. M., Moreno, R., et al. 2011, *A&A*, 536, L2  
 de Graauw, T., Helmich, F. P., Phillips, T. G., et al. 2010, *A&A*, 518, L6  
 de Val-Borro, M., Hartogh, P., Crovisier, J., et al. 2010, *A&A*, 521, L50  
 DiSanti, M. A., Bonev, B. P., Villanueva, G. L., et al. 2012, *Asteroids, Comets, Meteors 2012*, 16–20 May 2012, Niigata, Japan  
 Dones, L., Weissman, P. R., Levison, H. F., & Duncan, M. J. 2004, *Comets II*, 153  
 Eberhardt, P., Reber, M., Krankowsky, D., & Hodges, R. R. 1995, *A&A*, 302, 301  
 Hartogh, P., Lellouch, E., Crovisier, J. et al. 2009, *P&SS*, 57, 1596  
 Hartogh, P., Crovisier, J., de Val-Borro, M., et al. 2010, *A&A*, 518, L150  
 Hartogh, P., Lis, D. C., Bockelée-Morvan, D., et al. 2011, *Nature*, 478, 218  
 Hersant, F., Gautier, D., & Huré, J.-M. 2001, *ApJ*, 554, 391  
 Irvine, W. M., Schloerb, F. P., Crovisier, J., Fegley, B., Jr., & Mumma, M. J. 2000, *Protostars and Planets IV*, 1159  
 Jehin, E., Manfroid, J., Hutsemékers, D., Arpigny, C., & Zucconi, J.-M. 2009, *Earth Moon and Planets*, 105, 167  
 Kavelaars, J. J., Mousis, O., Petit, J.-M., & Weaver, H. A. 2011, *ApJ*, 734, L30  
 Levison, H. F., Duncan, M. J., Brasser, R., & Kaufmann, D. E. 2010, *Science*, 329, 187  
 McKeegan, K. D., Aléon, J., Bradley, J., et al. 2006, *Science*, 314, 1724  
 McKeegan, K. D., Kallio, A. P. A., Heber, V. S., et al. 2011, *Science*, 332, 1528

- McNaught, R. H., & Garrad, G. J. 2009, IAU Circ., 9062, 2  
Nakano, S. 2012, note NK 2216, <http://www.oaa.gr.jp/~oaacs/nk.htm>  
Paganini, L., Mumma, M. J., Villanueva, G. L., et al. 2012, ApJ, 748, L13  
Pilbratt, G. L., Riedinger, J. R., Passvogel, T., et al. 2010, A&A, 518, L1  
Roelfsema, P. R., Helmich, F. P., Teyssier, D., et al. 2012, A&A, 537, A17  
Villanueva, G. L., Mumma, M. J., DiSanti, M. A., et al. 2012, Icarus, in press  
Walsh, K. J., Morbidelli, A., Raymond, S. N., O'Brien, D. P., & Mandell, A. M. 2011, Nature, 475, 206  
Zakharov, V., Bockelée-Morvan, D., Biver, N., Crovisier, J., & Lecacheux, A. 2007, A&A, 473, 303
- 

- <sup>1</sup> LESIA, Observatoire de Paris, CNRS, UPMC, Université Paris-Diderot, 5 place Jules Janssen, 92195 Meudon, France  
e-mail: dominique.bockelee@obspm.fr  
<sup>2</sup> Dept. of Physics & Astronomy, University College London, Gower Street, London WC1E 6BT, UK  
<sup>3</sup> RAL Space, Science & Technology Facilities Council, Rutherford Appleton Laboratory, Chilton, Didcot, Oxon OX11 0QX, UK  
<sup>4</sup> Max Planck Institute for Solar System Research, Max-Planck-Str. 2, 37191 Katlenburg-Lindau, Germany  
<sup>5</sup> California Institute of Technology, Pasadena, USA  
<sup>6</sup> Space Research Centre, Polish Academy of Science, Warszawa, Poland  
<sup>7</sup> European Space Astronomy Centre, Madrid, Spain  
<sup>8</sup> Joint Astronomy Centre, 660 N. Aohoku Place, Hilo, HI 96720, USA  
<sup>9</sup> Institute for Space Imaging Science, Department of Physics and Astronomy, University of Lethbridge, Lethbridge, Alberta, Canada, T1K 3M4



## Appendix A: Data reduction and HIFI calibration

The comet was tracked using an up-to-date ephemeris provided by the JPL Horizons system. The *Herschel* rms pointing accuracy is approximately  $1''$ .

The data were reduced to level 2 products using the *Herschel* Interactive Processing Environment (HIPE 7.3). All lines were observed in the two orthogonal H and V polarizations. The two orthogonal polarizations were averaged. Note that the two polarizations are observed with different mixers, and their respective apertures are imperfectly co-aligned. The beam offset for the H and V average spectra is  $\sim 4''$  with respect to the pointed position.

The line intensities integrated over velocity were computed on the main-beam brightness-temperature scale using beam efficiencies of 0.75 and 0.73 for bands 1a and 4a, respectively, and a forward efficiency of 0.96. Based on the calibration error budget (Roelfsema et al., 2012), a conservative value for the uncertainty in the absolute intensity calibration is 10% for both bands. Most sources of errors are eliminated when comparing band 1a data, and the relative uncertainty is at most 5% in this case (sideband ratio, hot-load coupling, and temperature). Finally, the calibration uncertainty for the ratio of band 1a to band 4a lines is 10%.

## Appendix B: Water production rate: comparison with other measurements

Water production rates measured for C/2009 P1 (Garrad) from September to October 2011 are shown in Fig. 5. Reported values include retrievals from OH 18-cm observations (Colom et al. 2011, and in preparation), OH narrowband photometry (Schleicher et al., personal communication), and near-IR observations of water (DiSanti et al. 2012, Paganini et al. 2012; Villanueva et al. 2012). *Herschel*/HIFI and OH 18-cm observations, which were acquired close in date, provide consistent values. The data suggest that the activity of comet Garrad underwent significant variations, and reached a maximum at the time the HIFI observations were performed. The 987 GHz  $\text{H}_2\text{O}$  line observed with HIFI was also observed on 16 October 2011 with the Spectral and Photometric Imaging Receiver (SPIRE) aboard *Herschel*; the line intensity is  $\sim 40\%$  weaker than on 6 October 2011, when the HIFI measurements were conducted (Swinyard et al., in preparation), implying a water production rate consistent with the value measured from OH narrowband photometry on 18 and 20 October 2011 (65 days before perihelion, Fig. 5). The low values derived from the near-IR measurements, compared to other measurements, possibly reflect sublimation from short-lived icy grains in the inner coma since the field-of-view for these observations was much smaller (by a factor of ten or more) than for the other techniques.

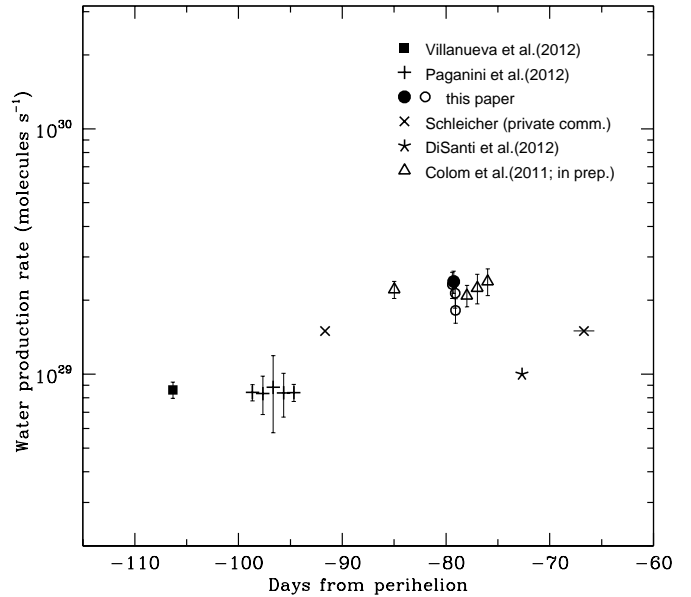


**Fig. 5.** Water production rates measured pre-perihelion in comet C/2009 P1 (Garrad). The time is with respect to the perihelion (23 December 2011). The plain and empty circles correspond to the 6-October single-point and mapping HIFI observations, respectively, analysed with the model with  $T_{\text{law}}$ .